JOURNAL OF MATERIALS SCIENCE 16 (1981) 1458–1470

Solid-state extrusion of nylons 11 and 12: processing, morphology and properties

WILLIAM G. PERKINS*, ROGER S. PORTER
Polymer Science and Engineering Department, Materials Research Laboratory, University of Massachusetts, Amherst, Massachusetts 01003, USA

Monofilaments of poly(11-amino-undecanoic acid) (nylon 11), and poly(laurylactam) (nylon 12) have been produced using solid-state extrusion methods in an Instron capillary rheometer. The resulting morphology, physical and mechanical properties were investigated. For nylon 11, at an extrusion ratio (ER) of 12, the crystalline melting-point temperature increased by 16° C, over the undrawn material, while the per cent crystallinity, X_c, increased by 23%. Nylon 12, extruded to a maximum ER of 6, realized an increase in T_m of 4° C at ER = 5 and an X_c increase of 14%. Young's modulus for nylon 11 increased from 3 GPa at an ER = 3 to 5.5 GPa at an ER = 7 and levelled off at greater ER. For nylon 12, the Young's modulus climbed from 2.5 GPa at ER = 3 to about 3.3 GPa at ER = 5.5. Conventionally melt-spun and cold-drawn nylon 11 and nylon 12 fibres exhibited Young's modulus values of 2.7 GPa and 2.9 GPa respectively. Atmospheric moisture loss was found not to affect solid-state extrusion of these higher nylons. Increases in extrusion temperature and/or pressure increased the extrusion rate. The flow activation energy of nylon 11 was 73 kcal mol^{-1} at 0.24 GPa extrusion pressure, and 124 kcal mol^{-1} at 0.49 GPa extrusion pressure. Calculated apparent viscosities were about 10^{14} poise and 10^{15} poise, respectively. The morphologies were shown by electron microscopy to be microfibrillar and the resulting monofilaments were transparent to visible light.

1. Introduction

Solid-state extrusion of high-density polyethylene has provided films and fibres of exceptionally high modulus and tensile strength [1, 2]. It was thought that studies with the hydrogen-bonded nylons would extend the art of crystalline-state extrusion into polymers with higher melting points. The higher nylons were chosen for initial studies because of their longer olefinic segments.

This study involves the process–structure–property relationships of nylon 11 [poly(11-amino-undecanoic acid)] and nylon 12 [poly(laurylactam)] extruded in the crystalline state. Discussion of results is divided into parts on nylon 11 and on nylon 12.

2. Experimental procedure

Solid-state extruded nylon morphologies were prepared in an Instron capillary rheometer by the technique detailed previously [3]. Variations on the process included crystallization and extrusion at several temperatures and pressures, as well as extrusion at constant rates (fixed cross-head speed) up to a predetermined maximum pressure. When the maximum pressure was attained, the load was cycled between narrow limits to maintain a near constant pressure.

Differential scanning calorimetry (DSC) was performed on the starting nylons and extrudates with a Perkin–Elmer DSC-1B at a heating rate of 10° C min^{-1} in order to determine heats of fusion (converted to per cent crystallinity, X_c) and crystalline melting-point temperatures, T_m. Entropy of fusion was calculated from the above parameters through their thermodynamic relationship.

A Perkin–Elmer TMS-1 thermomechanical ana-

*Present address: Goodyear Tire and Rubber Co., Akron, Ohio, USA.

 0022–2461/81/061458–13$03.30/0

lyser attachment to the DSC-1B machine was used for measurement of the linear expansion coefficient. Sample preparation for this test was as previously described [4]. A load of 3 g was used with the expansion probe, and the scanning rate was 10 ° C min^{-1}. For the tests, samples of approximate length 1 cm were used. Scans were made over a temperature range from − 140° C up to 190° C.

For studies of fibre mechanical properties, an Instron tensile testing machine, model TTCM, equipped with a 10 mm strain-gauge extensometer, was used. Load–elongation curves were obtained at room temperature using a fixed elongation rate for the modulus measurements of 0.02 cm min^{-1} and 0.50 cm min^{-1} for determination of tensile strength and strain-at-break. Samples were gripped in special clamps, described elsewhere [1], to prevent slippage in the jaws. Nevertheless, slippage occurred during testing of nylon 11 ultimate properties, rendering impossible determination of its tensile strength and the strain-at-break. Strain rates for the determination of Young's modulus and tensile strength (for nylon 12) were 3.33×10^{-4} sec^{-1} and 1.67×10^{-3} sec^{-1}, respectively. The Young's modulus was determined as the tangent to the stress–strain curve at 0.2% strain.

Dilute solution viscosity measurements were conducted in a silicone oil bath using a Number 100 Ubbelohde viscometer. The solvent was *m*-cresol and the test temperature was 50° C. Efflux time for the solvent was about 300 sec.

2.1. Nylon 11

2.1.1. Introduction

The nylon 11 used was supplied by the Rilsan Corporation, Glen Rock, New Jersey, having a weight average molecular weight, $\bar{M}_w = 34\,000$ and mean molecular number, $\bar{M}_n = 13\,000$. The crystalline melting-point temperature of the as-received material was found to be 189° C and the heat of fusion was found to be 11.26 cal gm^{-1}. This corresponds to approximately 21% crystallinity, as the heat of fusion for 100% crystalline nylon 11 has been calculated to be 53 cal gm^{-1} [5, 6].

The principal crystal structure of nylon 11 has been investigated [7–9] and found to exist in a planar zig-zag conformation. The unit cell contains one monomer unit and is triclinic, having dimensions: $a = 4.9$ Å, $b = 5.4$ Å, c (chain axis) = 14.9 Å; and having characteristic angles: $\alpha = 49°$, $\beta = 77°$, $\gamma = 63°$ [7]. Polymorphism exists in nylon 11 as it does in virtually all the polyamides. Above 70° C, Genas [8] found that the *a*–*b*(basal) plane of the triclinic cell assumes pseudo-hexagonal packing. Onogi, *et al.* [9] observed that quenched films of nylon 11 contain γ-phase (pseudo-hexagonal) crystals, whereas films solution-cast from *m*-cresol contain α-phase (triclinic) crystals. When films containing γ-phase crystals were annealed at temperatures above 90° C, they transformed into the α-modification. This $\gamma \rightarrow \alpha$ transformation can also occur on stretching [10].

Fig. 1a is a wide-angle X-ray photograph of a nylon 11 extrudate solid-state extruded to an extrusion draw ratio of 7. The diffraction pattern is consistent with that for the α-phase (triclinic) modification. It has been suggested [11] that the "parallel" structure of nylon 11, wherein the polar amide groups are tilted with respect to the chain axes, represents a stronger hydrogen bond association than does the "antiparallel" modification. This is consistent with the triclinic unit cell generally observed at room temperature [7–9]. The parallel modification arises when neighbouring chains all lie in the same direction. In the antiparallel form, the chains alternate in direction. There is a difference between the two forms because the sequence of chain atoms encountered along the chain in one direction for ω-amino acid polyamides is the reverse of that found in the opposite direction [12]. For the "odd" ω-amino acid nylons, such as nylon 11, both the parallel and anti-parallel forms allow complete hydrogen bonding [7, 13]. Such is not the case for the "even" ω-amino acid nylons (e.g. nylon 12), discussed in Section 2.2.

The effects of pressure on the crystallization and structure of nylon 11 have been reported [14, 15]. Gogolewski and Pennings [14] found that pressures exceeding 0.29 GPa (3 kbar) and temperatures higher than 230° C are sufficient for the growth of chain-extended crystals, either by pressure-induced crystallization from the melt or by annealing of the folded-chain crystals. They note that the α-phase (triclinic) crystalline modification, commonly found for folded-chain crystals of nylon 11, was preserved in the high pressure crystallization and annealing experiments. They concluded that, during the initial stages of crystallization under pressure, folded-chain crystals are formed, with a crystalline order and long spacing greater than that of the starting nylon 11. These

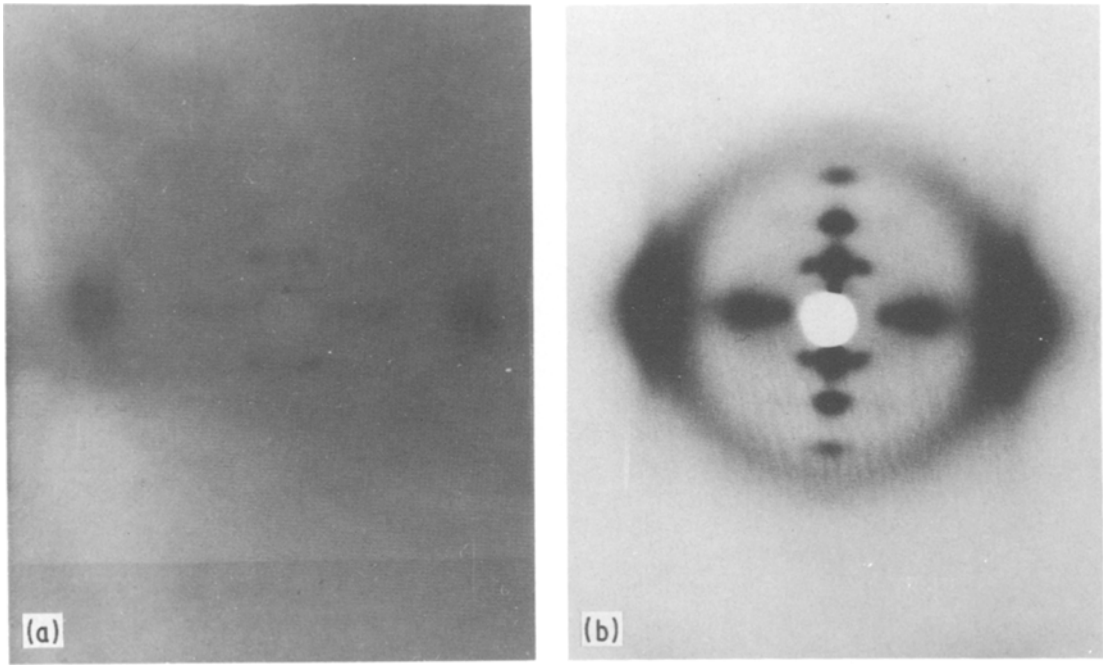

Figure 1 Wide-angle X-ray photographs of (a) nylon 11 and (b) nylon 12 solid-state extruded fibres. Fibre axis vertical.

authors noted a melting-point temperature increase with pressure of 160° C GPa^{-1} (16° C $kbar^{-1}$).

Newman *et al.* [15] performed a detailed X-ray structure analysis on nylon 11 at various temperatures and pressures. They concluded that the chain conformation of Slichter [7] was distorted (shortened) along the *c*-axis at ambient temperature and pressure. No phase transformations from the α-phase crystal structure were observed at room temperature up to pressures of 1.9 GPa (19.5 kbar). However, a crystal transition at atmospheric pressure was observed at 95° C: the triclinic (α-phase) changing to a pseudo-hexagonal structure. It was found that the increase in transition temperature with pressure was about 150° C GPa^{-1} (15° C $kbar^{-1}$).

Differential thermal analysis (DTA) measurements by Gordon [16] showed that the commonly-observed glass transition at 43° C disappears if a sample is annealed at 75° C for 24 h. Instead, a transition appeared at 92° C. However, after 3 days at room temperature, samples showed transitions at both 40 and 92° C. He concluded that the type of hydrogen-bonded network formed from the melt depends on the temperature of formation and that the break-up of such networks is responsible for the observed glass transitions. He postulated that the network formed at the (ambient) annealing temperature is relatively stable, but the continuing motion of the paraffinic segments leads to generation of another network.

Further work on transitions in nylon 11 was reported by Northolt, *et al.* [17]. Results from DSC, tensile testing and wide-angle X-ray diffraction measurements on orientated samples aged at various temperatures revealed that the glass transition in nylon 11 shifted to higher temperatures as samples were aged at progressively higher temperatures. This was seen as resulting from amorphous-phase hydrogen-bond weakening at the higher (ageing) temperatures and their subsequent orientation and reformation. No effect of moisture on transitions was reported.

The presence of several relaxations in nylon 11 has been observed by Onogi, *et al.* [9] in dynamic mechanical spectra. They suggest that the primary relaxation, that is the glass transition, is at approximately 70° C with a smaller relaxation at −50° C. Another relaxation is seen at about 160° C. This dispersion may be analogous to the α-transition seen in polyethylene from 80 to 100° C [18].

2.1.2. Experimental results

The effect of extrusion temperature and pressure on the extrusion rate is shown in Fig. 2. This is a plot of extrudate length against extrusion time

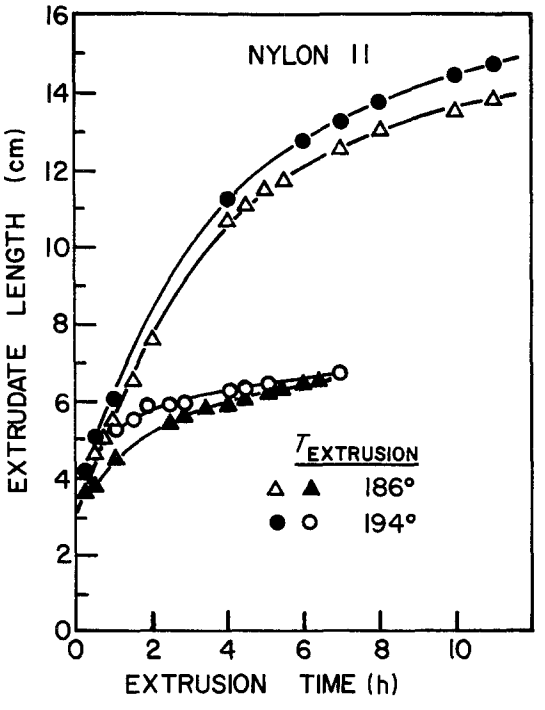

Figure 2 Extrudate length plotted against extrusion time for nylon 11 fibres crystallized and extruded at pressures of 0.24 GPa (lower curves) and 0.49 GPa (upper curves) and at the temperatures shown.

at two temperatures and pressures. The extrusion pressure in the lower time curves is 0.24 GPa (2400 atm). As expected, the higher extrusion temperature results in an initially higher extrusion rate. However, both extrusion rates reduce with time and tend to zero. The upper curves in Fig. 2 show the effect of extrusion temperature on extrusion rate at a (maximum) extrusion pressure of 0.49 GPa (5000 atm). Although the initial extrusion rate is also slightly higher at higher extrusion temperature, at long times the two (extrudate length against extrusion time) curves diverge; at the lower pressure the two curves converge. Also, at the higher pressure, the curves at both extrusion temperatures do not tend to zero at long times, although their slopes are decreasing.

Table I shows the results of dilute-solution viscosity measurements on both virgin nylon 11 pellets and on fibres extruded at several temperatures. The lack of viscosity change with time, at any extrusion temperature, indicates that the polymer did not undergo degradation during extrusion.

The effect of moisture content on the extrusion rate of nylon 11 is shown in Fig. 3. One sample

TABLE I Relative viscosities of nylon 11 fibres extruded at varying temperatures and dissolved in *m*-cresol (0.37 g dl^{-1} concentration) at 50° C

Extrusion temperature (°C)	Relative viscosity
Virgin pellets	1.14
186	1.16
190	1.21
194	1.13
198	1.23

(shown by the circles in Fig. 3) was dried in a vacuum oven at 100° C for 24 h then stored in a desiccator over P_2O_5. The other (shown by the triangles in Fig. 3) had no conditioning prior to processing. All the points fall on the same curve, indicating a negligible effect of adsorbed water on extrusion rate. A third sample was immersed in steam at atmospheric pressure for 71 h. Upon removal of the restrictor at the beginning of extrusion, the extrusion pressure immediately dropped toward zero and a foamed melt rapidly extruded.

The effect of pulling on the emerging extrudate is shown in Fig. 4. Nylon 11 was extruded at 0.49 GPa and 194° C and a 5 kg weight was attached to the extrudate. The initial extrusion rate was some-

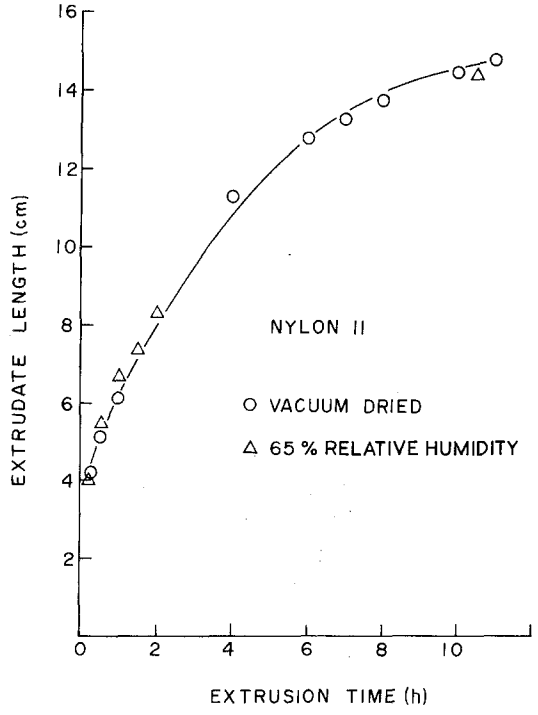

Figure 3 Extrudate length plotted against extrusion time for nylon 11 fibres both vacuum dried (circles) and non-dried (triangles) prior to processing. Crystallized at 194° C and 0.24 GPa; extruded at 194° C and 0.49 GPa.

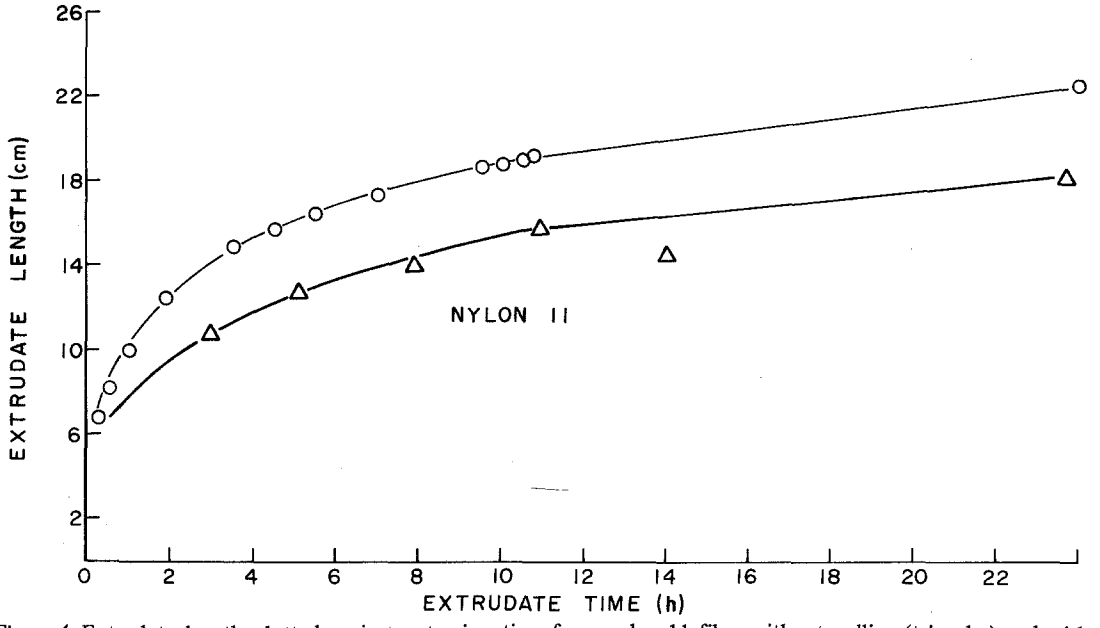

Figure 4 Extrudate length plotted against extrusion time for a nylon 11 fibre without pulling (triangles) and with a 5 kg weight attached to the emerging extrudate (circles). Crystallized at 194° C and 0.24 GPa; extruded at 194° C and 0.49 GPa.

what faster than that found to result from the same conditions without attached weights. However, at long times no significant increase in extrusion rate was observed as a result of pulling.

Figs 5 to 7 illustrate several physical properties of solid-state extruded nylon 11 and their relationship to the extrusion (draw) ratio (ER). Fig. 5 shows a rise in T_m, with ER up to about 205° C at an ER of 12. This represents a 16° C increase over the undrawn virgin material (ER = 1). Per cent crystallinity, X_c, as measured by DSC against ER measurement, is shown in Fig. 6. Crystalline content also increases significantly with ER from about 21% to about 44% at an ER of 10. At an ER of 12, the lower values may be experimental error. Fig. 7 shows that the entropy of fusion, ΔS_f, rises steeply to ER = 3 and then approaches a limit.

Fig. 8 is a plot of Young's modulus agains ER. The maximum value of about 5.5 GPa was attained at an ER of 7 and thereafter the Young's modulus remained constant. This compares with a Young's modulus of 1.3 GPa exhibited by injection-molded parts, and 2.7 GPa obtained from commercially spun and drawn filaments.

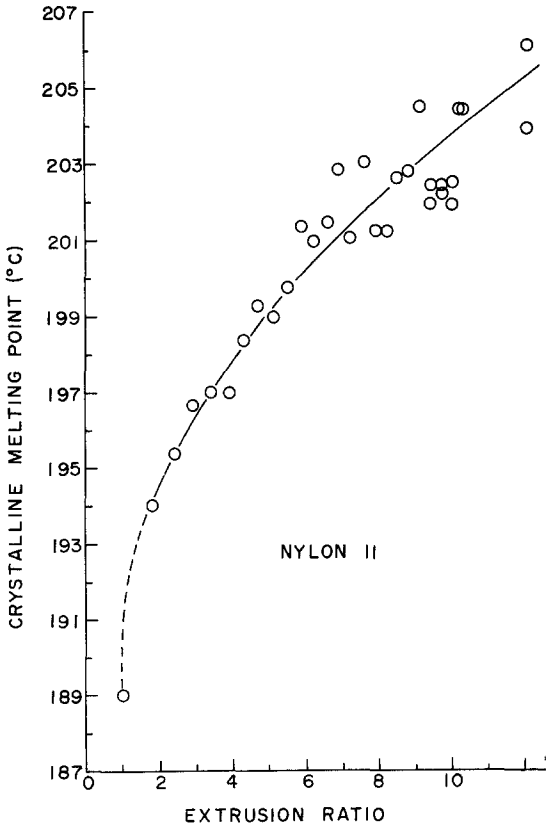

Figure 5 Crystalline melting point plotted against extrusion ratio (ER) for a nylon 11 fibre crystallized at 194° C and 0.24 GPa; extruded at 194° C and 0.49 GPa. ER = 1 is undrawn material.

2.2. Nylon 12

2.2.1. Introduction

The nylon 12 used in this study was supplied by Dr Akiro Kishimoto of the Toyo Seikan Company

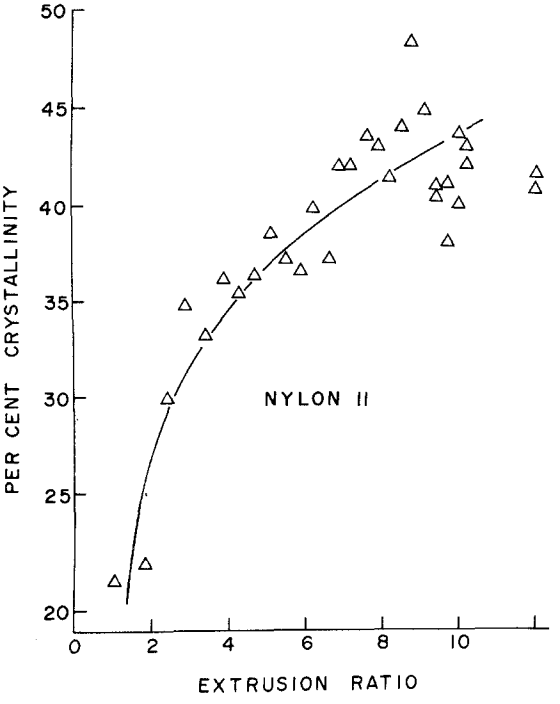

Figure 6 Per cent crystallinity plotted against ER for nylon 11 fibre crystallized at 194° C and 0.24 GPa; extruded at 194° C and 0.49 GPa. ER = 1 is undrawn material.

Ltd, Yokohama Japan, having a reported $\bar{M}_w \simeq 28\,600$ and a $\bar{M}_n = 14\,300$. The crystalline melting-point temperature of the as-received material was 179° C and the heat of fusion was 10.0 cal gm^{-1} corresponding to 18.5% crystallinity as the heat of fusion for 100% crystalline nylon 12 has been reported to be 54 cal gm^{-1} [6].

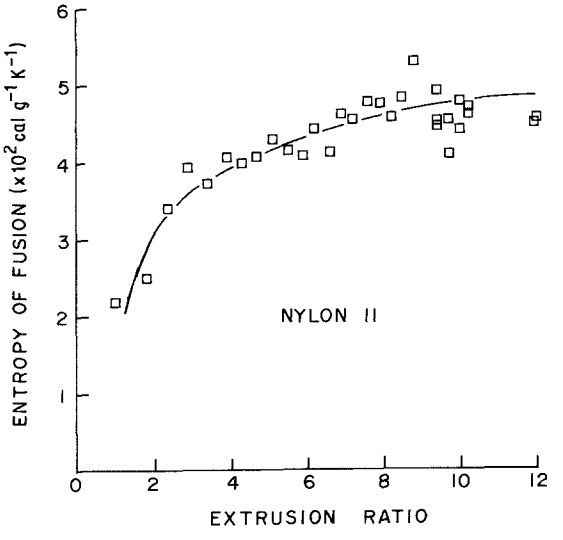

Figure 7 Entropy of fusion plotted against ER for a nylon 11 fibre crystallized at 194° C and 0.24 GPa, extruded at 194° C and 0.49 GPa. ER = 1 is undrawn material.

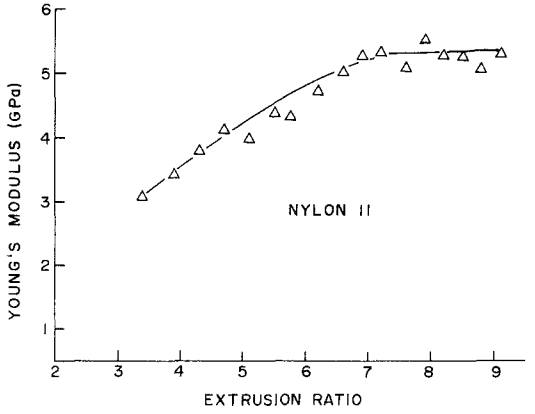

Figure 8 Young's modulus plotted against ER for a nylon 11 fibre crystallized at 194° C and 0.24 GPa; extruded at 194° C and 9.49 GPa.

The crystal structure of nylon 12 has been found [19, 20] to be a γ-phase modification wherein the chains are twisted about the methylene groups. The conformation is planar zig-zag. Inoue and Hoshino [20] prepared a sample by drawing a monofilament to 3.6 times its length (3.6×) in boiling water then annealing it at 160° C for 10 h. They found it showed monoclinic unit cell resembling the γ-form of the other even nylons. From X-ray data they calculated the monoclinic unit cell dimensions to be: $a = 9.38$ Å, $b = 32.2$ Å (fibre axis) and $c = 4.87$ Å; and of characteristic angle: $\beta = 121.5°$. There are four repeat monomer units per unit cell. Northolt, *et al.* [19], found that nylon 12 may exist in two different forms: melt-pressed sheet, quenched in ice water, drawn 4.5× at room temperature, and annealed at 170° C at constant length for several hours under nitrogen, revealed a hexagonal unit cell and melt-pressed sheet, quenched in ice water, drawn 7× at just under 180° C and cooled under stress to room temperature, exhibited what appeared to be a mixture of mono- and triclinic unit cell structures. No transition to the α-form, wherein chains are antiparallel, was observed for nylon 12 upon stretching or treatment with aqueous phenol. It was therefore concluded that the γ-form of nylon 12 was more stable than that for nylon 6, nylon 8 or nylon 10. This led to the conclusion that the longer the molecular chain in the even nylons, the more the crystal shows a tendency to form the γ-phase [20, 21]. Nylon 12 is always found in the "parallel" modification [13] in which neighbouring chains all lie in the same direction; because this would result in 50% free NH-groups, a twisting of the molecule

is necessary for the observed complete hydrogen bond formation. This twisting causes a shortening of the unit cell along the chain (b) axis and results in the γ-form of the crystal. The wide-angle X-ray diffraction pattern shown in Fig. 1b is a typical pattern for the γ-phase of the even nylons. The strong intensity of the meridional diffraction spots results from the carbonyl oxygen atoms all lying in planes perpendicular to the fibre axis [21].

Crystallization and annealing under a high pressure of 0.48 GPa (4.9 kbar) was carried out by Stamhuis and Pennings [22]. They noted that a partial transformation of the pseudo-hexagonal or monoclinic γ-crystal structure to an α-phase modification occurred in samples crystallized at 240° C and 0.48 GPa for 16 h. In the pressure range up to 0.29 GPa (3 kbar) the increase in melting temperature was about 200° C GPa^{-1} (20° C $kbar^{-1}$), whereas at a pressure of 0.78 GPa (8 kbar), the relationship was found to be 120° C GPa^{-1} (12° C $kbar^{-1}$). The authors observed no chain-extended crystals, although a broadening of the distribution of crystal dimensions was noted at the higher crystallization pressures.

Onogi, *et al.* [9] found no evidence of an α-type relaxation for nylon 12 (as for polyethylene) by dynamic mechanical tests, such as they did for nylon 11 at about 160° C.

2.2.2. Experimental results

The effect of extrusion temperature on extrusion rate is shown in Fig. 9. The initial rate is higher at the higher temperature but after 15 minutes the rates are both slower and are equivalent. At longer extrusion times, the low-temperature extrusion rate begins to level off, while the higher temperature extrusion rate continues to increase, albeit more slowly than at short times.

Fig. 10 shows the effect of the crystallization/extrusion pressure on the crystalline melting-point temperature, T_m, and on the per cent crystallinity, X_c, of solid-state extruded nylon 12. The crystallization and extrusion pressures are equal and, as shown in Fig. 10, T_m decreases linearly with extrusion pressure from 0.12 to 0.24 GPa, then remains constant; per cent crystallinity rises steadily with extrusion pressure to 0.24 GPa before levelling off.

The influence of crystallization/extrusion temperature on the crystalline melting point temperature and the degree of crystallinity for nylon 12 fibres is shown in Fig. 11. The crystallization and extrusion temperatures were equal and, as shown, the melting point temperature increased by about 3° C as the crystallization/extrusion temperature was increased from 176 to 196° C. The degree of crystallinity rises from about 19% to about 30% for an increase in the crystallization/extrusion temperature of 8° C, then levels off at higher preparation and extrusion temperatures.

Fig. 12 shows an increase in T_m from 179° C for undrawn material (ER = 1) to 183° C for fibres extruded to an ER of about 5; the crystallinity increased from 19% from undrawn to 33% for extrudates drawn to about 6 ×. Both curves indicate significant increases in crystalline perfection with increasing ER.

Fig. 13 shows that the entropy of fusion, ΔS_f,

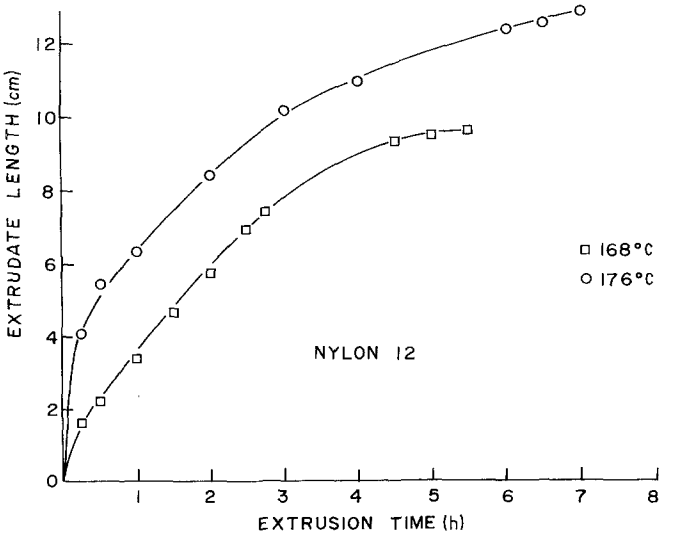

Figure 9 Extrudate length plotted against extrusion time for nylon 12 fibres crystallized at 184° C and 0.24 GPa, extruded at 0.49 GPa and at the temperatures shown.

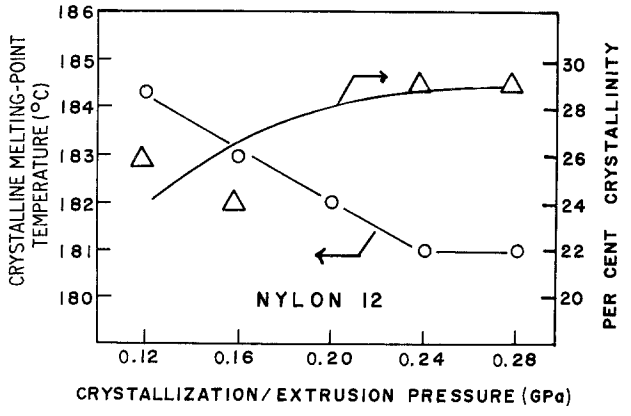

Figure 10 Crystalline melting point and per cent crystallinity plotted against crystallization/extrusion pressure for nylon 12 fibres. Crystallization/extrusion temperature: 178° C. Measurements taken at an ER of 4.

exhibits an initial sharp increase with increasing ER followed by a more gradual increase at higher values.

Thermomechanical analyses (TMA) were performed on nylon 12 fibres at an ER of 5 (Fig. 14). This is a semi-logarithmic plot of the normalized change in length of the fibre, i.e. orientation direction, against scanning temperature. The upper curve is for a melt-extruded (disorientated) fibre whereas the bottom curve depicts the behaviour of a solid-state extruded fibre (ER = 5) of the same nylon 12. The melt-extruded fibre has a large positive expansion coefficient (slope of the curve) up to the melting point at 179° C. The solid-state extruded fibre has a smaller positive expansion coefficient up to − 70° C, then contracts rapidly on further heating. Results of temperature cycling in the TMA experiment are shown in Fig. 15 and are discussed in Section 3.

Fig. 16 shows the change in Young's modulus with ER. For an increase in ER from 3 to 5.5, the tensile modulus gradually increased from 2.6 to 3.3 GPa. Mechanical data are compared in Table II for moulded, commercially melt-spun and cold-drawn, and solid-state extruded (ER = 5.5) samples.

3. Discussion and conclusions

3.1. General

Several factors come into play during the solid-state extrusion of nylon. As with other polymers, strain hardening (defined below) plays an important role, as does molecular weight and the conditions of preparation of morphology prior to extrusion. Nylon extrusion is also affected by the hydrogen bonding of amide groups between chains. These bonds have a dissociation energy of about 8 kcal mol^{-1} and serve to tie nylon molecules together. They exist in the non-crystalline as well as crystalline regions of nylons [25].

The influence of intermolecular hydrogen bonding on the flow of polymer melts has been investigated [26] with co-polymers of ethylene and acrylic and methacrylic acids. An interesting result is that an increase in the degree of hydrogen bonding substantially enhances both the flow activation

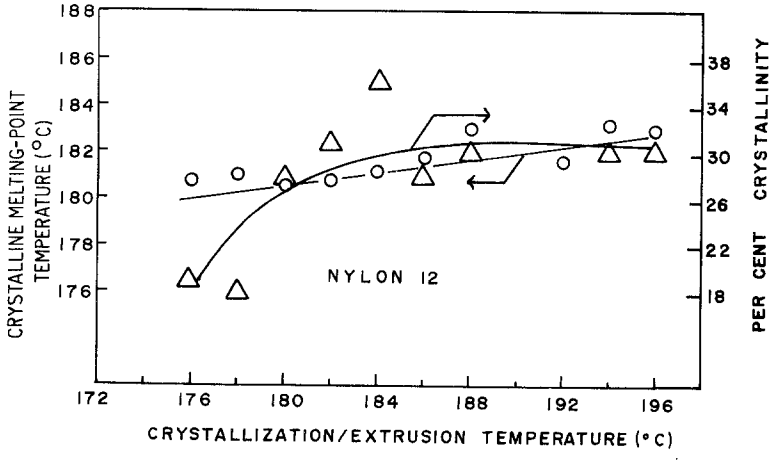

Figure 11 Crystalline melting point and per cent crystallinity plotted against crystallization/extrusion temperature for nylon 12 fibres. Crystallization/extrusion pressure: 0.24 GPa. Measurements taken at an ER of 4.

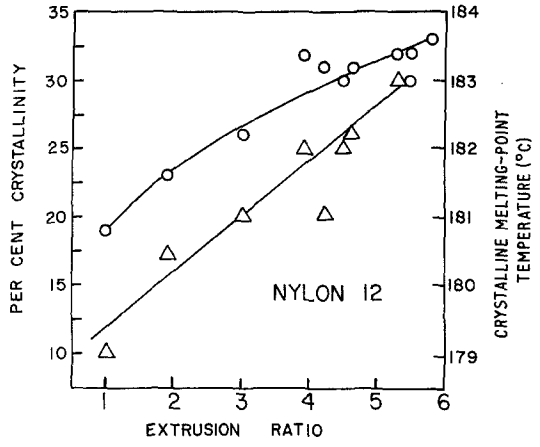

Figure 12 Crystalline melting point and per cent crystallinity plotted against ER for nylon 12 fibres crystallized and extruded at 178° C and 0.24 GPa. ER = 1 is undrawn material.

energy and the viscosity. In this sense, the lower nylons, such as nylon-66 and nylon-6, may be difficult to solid-state extrude because of their abundant hydrogen bonding which inhibits sliding displacement along consecutive hydrogen-bonded planes, a common deformation mode [27].

The effect of pressure on hydrogen bonding has not been widely investigated but there is evidence [28] that increasing pressure causes a decrease in the distance between the planes containing the hydrogen bonds as well as between the planes held by van der Waals interactions. This compressed structure would also be likely to retard flow in solid-state extrusion.

Flow activation energies, E_a, were calculated for nylon 11 in this study at two extrusion pressures using the equation

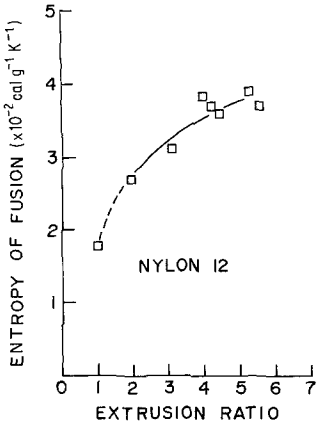

Figure 13 Entropy of fusion plotted against ER for nylon 12 fibres crystallized and extruded at 178° C and 0.24 GPa. ER = 1 is undrawn material.

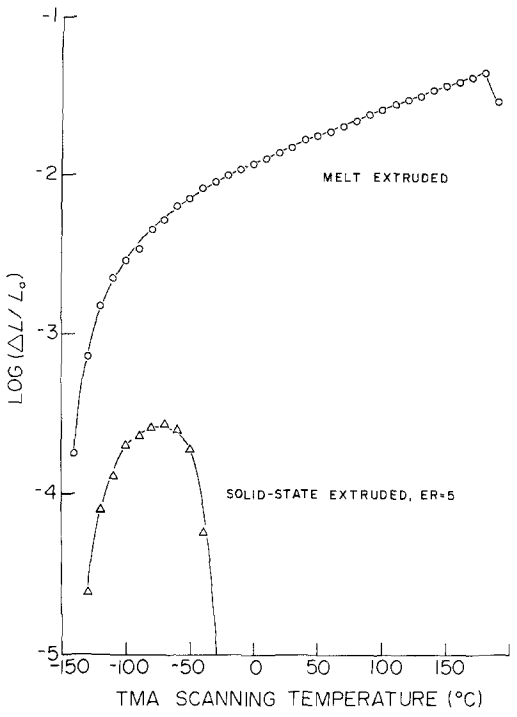

Figure 14 Linear expansion coefficients (slopes) of melt-extruded and solid-state extruded (ER = 5) nylon 12 fibres. Solid-state extruded fibre crystallized at 186° C and 0.24 GPa: extruded at 176° C and 0.49 GPa.

$$\frac{d(\ln \eta)}{d(T)^{-1}} = \frac{E_a}{R}, \tag{1}$$

where T is the extrusion temperature (in K), R is the gas law constant and η is the apparent viscosity, calculated from

$$\eta = \frac{\sigma}{\frac{dL}{dt} \cdot \frac{1}{L}}, \tag{2}$$

where σ is the shear (applied stress), dL/dt is the shear rate and L is the length of extrudate where the calculations were made.

The apparent activation energy doubled (73 to 124 kcal mol^{-1}) with a doubling of the extrusion pressure (0.24 to 0.49 GPa). Apparent viscosities during extrusions were calculated as about 10^{14} poise at 0.24 GPa extrusion pressure and about 10^{15} poise at 0.49 GPa, both measred at 190° C. High-density polyethylene extruded in the solid-state exhibits an apparent viscosity of between 10^{12} and 10^{13} poise. Mead and Porter [29] found the flow activation energy of a high-density polyethylene to be between 20 and 60 kcal mol^{-1} when the polymer was solid-state extruded at tem-

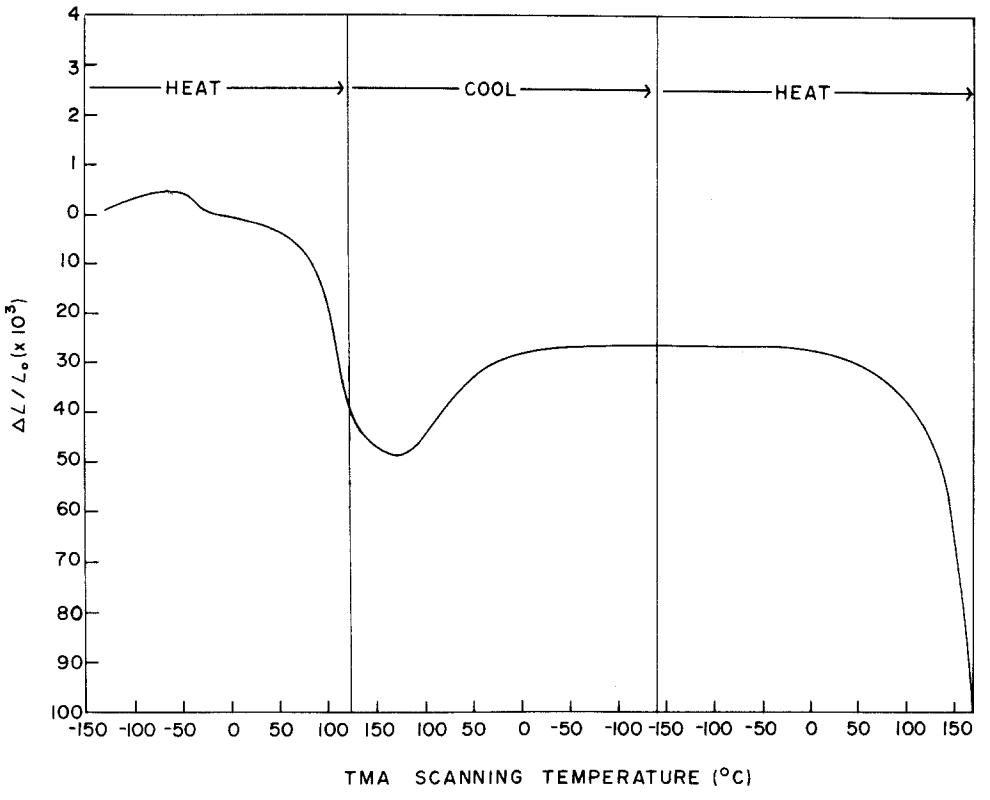

Figure 15 Temperature cycling of a nylon 12 fibre in the thermochemical analyser. Three cycles shown: heating, cooling and reheating. The slope of the plot at any point gives the linear expansion coefficient at that point.

peratures in the vicinity of the ambient melting point. Measurements were made at 0.24 GPa where the corresponding nylon 11 value was 73 kcal mol^{-1}.

Nylon 11 exhibits a transition at 160° C whereas nylon 13 shows no such high-temperature transition, as detected by dynamic mechanical testing [9]. This α-transition may well be responsible for the achievement of higher extrusion ratios and faster extrusion rates with nylon 11. Such relaxations are widely reported for other semi-crystalline polymers, including polyethylene. They are generally believed to result from the onset of motions within the crystalline phase. Hashimoto, *et al.* [30] believe that the α-transition in polyethylene results from orientation dispersion of crystallites accompanied by the shearing of mosaic crystallites within the lamellae and from molecular motion within the crystals. Other investigators have postulated kink [31, 32] or twist [33] crystal defect motions and chain rotation [34–36] as responsible for the observed α-relaxation in polyethylene. These

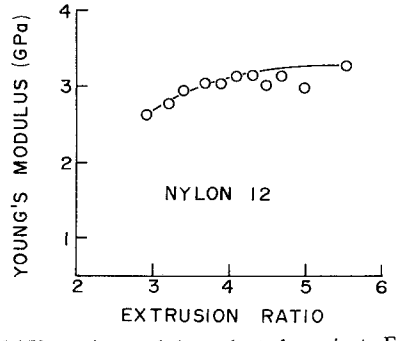

Figure 16 Young's modulus plotted against ER for a nylon 12 fibre crystallized at 184° C and 0.24 GPa and extruded at 182° C and 0.49 GPa.

TABLE II Comparison of mechanical properties of moulded, commercially melt-extruded/cold-drawn, and solid-state (cold) extruded nylon 12. The latter extruded at an ER of 5.5 and $\overline{M}_w = 28\,600$, $\overline{M}_n = 14\,300$

Sample preparation	Property		
	Tensile modulus (GPa)	Tensile strength (GPa)	Elongation-at-break (%)
Moulded (from [23])	1.24	0.06	300
Cold-drawn (from [24])	2.9	0.31	40
Cold-extruded	3.3	0.26	38

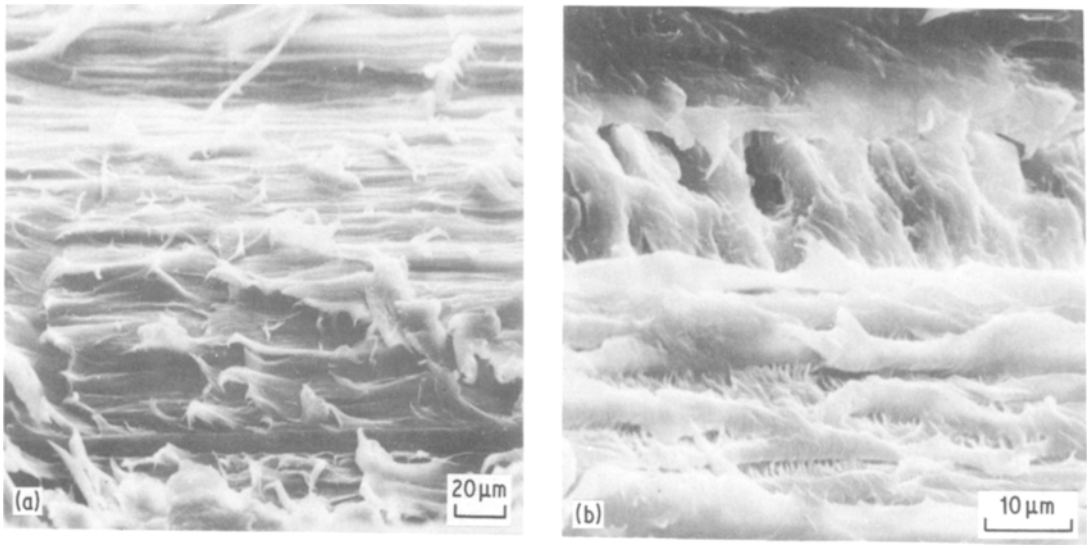

Figure 17 SEM photographs of solid-state extruded nylon 12 fibres fractured (peeled) under liquid nitrogen along a horizontal draw direction. ER = 7.

processes may actually occur in nylon 12 but be undetectable by dynamic mechanical testing due to their small magnitude [35]. In any case, such motions in the crystalline phase should aid the extrusion process by imparting mobility.

3.2. Strain Hardening

Strain hardening is a phenomenon which is commonly observed on drawing semi-crystalline polymers below their T_m temperature, and usually somewhat below their glass transition, T_g, temperature for amorphous polymers. During strain hardening the molecules become orientated parallel to the deformation direction. For semi-crystalline polymers such as the nylons, the original crystal lamellae are broken up during deformation and aligned by the orientation direction to form microfibrils [37, 38]. Figs 17 and 18 show scanning electron microscope (SEM) photographs of solid-state extruded nylon 12 extrudates fractured along the draw direction. Microfibrils can plainly be seen at each magnification.

With the high nominal-extrusion-ratio dies com-

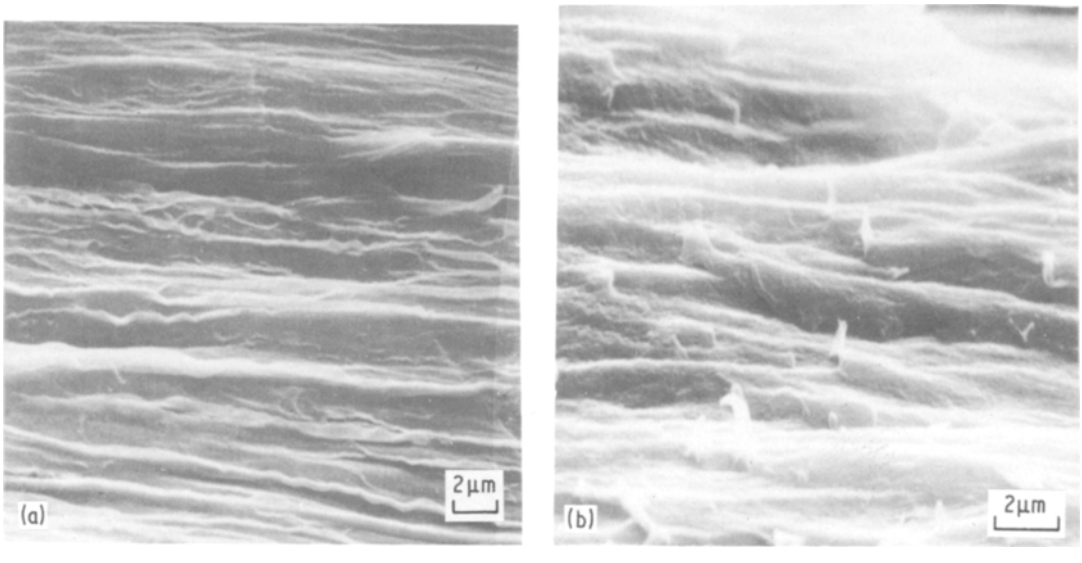

Figure 18 SEM photographs of solid-state extruded nylon 12 fibres shown at a higher magnification than that of Fig. 17.

monly used in this laboratory, the extrusion ratio (ER) of the extrudate increases with extrudate length. In the case of high-density polyethylene, maximum attainable ER is limited by a fracture mechanism at extrusion ratios greater than 40. The nylons investigated in this study also exhibited limiting extrusion ratios. Nylon 12 exhibited a maximum ER of about 7, and nylon 11 exhibited a maximum ER of about 12. In most cases, however, maximum ER were limited not by fracture of the extrudate, as in the case with polyethylene, but rather by the virual cessation of extrusion. In other words, after a long time ($>$ 8 hours), extrusion rates for the nylons declined to less than 1 mm hr^{-1}. Strain hardening of these polymers apparently reaches the point where even 0.49 GPa is insufficient pressure to force them through the die.

3.3. Pressure

The effect of crystallization pressure on nylons 11 and 12 has been investigated [14, 22]. The pressure range used in the present study for nylon 12 is below the pressure necessary for growth of extended chain crystals. The results presented here for nylon 12 indicate that, for the pressure range investigated, increasing crystallization/extrusion pressure causes a greater number of crystals to be formed, but crystals are smaller in size and/or perfection. One would expect such increases since the undercooling is less at higher crystallization temperatures at a given pressure. The results may differ for conditions where pressure can produce extended-chain crystals [22].

3.4. Melting behaviour

Both melting-point temperature and heat of fusion (here converted to per cent crystallinity) are related to the entropy of fusion by

$$\Delta G_f = \Delta H_f - T_m \Delta S_f, \quad (3)$$

where ΔG_f is the Gibbs free energy of fusion, ΔH_f is the enthalpy (heat) of fusion, T_m is the melting-point temperature (in K) and ΔS_f is the entropy of fusion. Tonelli [39] divides the entropy of fusion into two components: a constant volume contribution and a volume expansion contribution.

In the present study, the crystalline melting-point temperature increases more rapidly than the per cent crystallinity. This may result from the small increase in the entropy of fusion, plotted against extrusion ratio in Figs 7 and 13 for nylon 11 and nylon 12, respectively. Such variation in entropy is expected from Tonelli's conclusions since both nylon 11 and 12 are known to exhibit polymorphism at elevated temperatures and/or under conditions of solid-state deformation [7, 8, 15, 16, 19].

3.5. Thermomechanical analysis

Thermomechanical analysis (TMA) can be used as a qualitative measure of chain orientation and extension for measurements along the fibre direction. Solid-state extruded nylon 12 samples all showed an initial positive expansion coefficient that was smaller than that found for the corresponding melt-extruded sample (Fig. 14). As the scanning temperature was increased, solid-state extruded fibres irreversibly contracted in all cases at temperatures less than 0° C. The initial small positive coefficient of expansion is due to orientation and possibly a small proportion of extended-chain crystals which counteract the large positive coefficient arising from unorientated amorphous and folded-chain regions [40].

A solid-state extruded sample of nylon 12 was heated from $-130°$ C to 150° C in the thermomechanical analyzer and then cooled again to $-130°$ C followed by another heating cycle. The behaviour on initial heating was as described above. However, upon recooling, the sample at first expanded (in the axial direction), then reached a constant length which did not vary (with cooling and reheating) from $-25°$ C on the cooling cycle to about 0° C on heating cycle (see Fig. 15). Beyond this point, the sample shortened with increase in temperature up to the melting point, as reported earlier for solid-state extruded nylon 12. The plateau in Fig. 15 apparently results from annealing of the morphology during the first heating cycle during which hydrogen bonds are given sufficient mobility. The new structure is more stable and retains its dimensional stability up to about 0° C above which instability occurs. In the temperature range 0 to 150° C (during heating), the fibre behaviour is the same before and after thermal treatment. This state probably consists of unorientated amorphous and crystalline regions stabilized by hydrogen bonds, along with an orientated, and possibly an extended-chain, component which survives thermal annealing (at least up to 150° C).

3.6. Tensile modulus

Young's modulus of nylon 11 increases more

rapidly with draw than that of nylon 12. However, beyond an ER of 7, the nylon 11 modulus remains constant. Since the tensile modulus of high-density polyethylene begins to sharply increase only at extrusion ratios greater than 10, the potentially high mechanical properties of nylons may be realized only when higher ERs are attained. In any case, nylon 11 fibres cold-extruded in this study at an ER of 7 show an 80% increase in tensile modulus over commercial monofilaments. Nylon 12 fibres at an ER of 5.5. display a modulus equal to that of commercial monofilaments.

In conclusion, the nylons appear to offer the promise of highly improved physical and mechanical properties if higher extrusion ratios can be realized. By the incorportation of certain additives prior to crystallization and extrusion, this may be possible. Another possible approach may use the split-billet technique, recently developed in this laboratory [41]. In the present study, the measured mechanical tensile moduli for nylon 11 and nylon 12 are equal to or greater than those reported in the literature for these polymers. The melting point temperatures and degrees of crystallinity were significantly increased over the virgin material. Further work on nylon systems would seem to be indicated.

References

1. N. J. CAPIATI and R. S. PORTER, *J. Polymer Sci., Polymer Phys. Ed.* **13** (1975) 1177.
2. W. G. PERKINS, N. J. CAPIATI and R. S. PORTER, *Polymer Eng. Sci.* **16** (1976) 200.
3. N. J. CAPIATI, S. KOJIMA, W. G. PERKINS and R. S. PORTER, *J. Mater. Sci.* **12** (1977) 334.
4. R. S. PORTER, N. E. WEEKS, N. J. CAPIATI and R. J. KRZEWKI, *J. Thermal Anal.* 8 (1975) 547.
5. M. INOUE, *J. Polymer Sci.* **A-1** (1963) 3427.
6. R. GRECO and L. NICOLAIS, *Polymer* **17** (1976) 1049.
7. W. P. SLICHTER, *J. Polymer Sci.* **36** (1959) 259.
8. M. GENAS, *Agnew. Chem.* **74** (1962) 535.
9. S. ONOGI, K. ASADA, Y. FUKUI and I. TACHINAKA, *Bull. Inst. Chem. Res. Kyoto Univ.* **52** (1974) 368.
10. T. SASAKI, *J. Polymer Sci.* **B-3** (1965) 557.
11. W. O. BAKER and C. S. FULLER, *J. Amer. Chem. Soc.* **64** (1942) 2399.
12. R. HILL and E. E. WALKER, *J. Polymer Sci.* 3 (1948) 609.
13. F. W. LORD, *Polymer* **15** (1974) 42.
14. S. GOGOLEWSKI and A. J. PENNINGS, *Polymer* **18** (1977) 660.
15. B. A. NEWMAN, T. P. SHAM and K. D. PAE, *J. Appl. Phys.* **48** (1977) 4092.
16. G. A. GORDON, *J. Polymer Sci.* **A-2** (1971) 1693.
17. M. G. NORTHOLT, B. J. TABOR and J. J. VAN AARTSEN, *Prog. Colloid and Polymer Sci.* **57** (1975) 225.
18. R. BOYD, *A.C.S. Organic Coatings and Plastics Preprint* **35** (1975) 216.
19. M. G. NORTHOLT, B. J. TABOR and J. J. VAN AARTSEN, *J. Polymer Sci.* **A-2** (1972) 191.
20. K. INOUE and S. HOSHINO, *J. Polymer Sci., Polymer Phys. Ed.* 2 (1973) 1077.
21. D. C. VOGELSONG, *J. Polymer Sci.* **A-1** (1963) 1055.
22. J. E. STAMHUIS and A. J. PENNINGS, *Polymer* **18** (1977) 667.
23. "Modern Plastics Encyclopedia" Vol. 53 (1976–7) No. 10A, p. 465.
24. A. V. TOBOLSKY and H. F. MARK, (Eds), "Polymer Science and Materials" (Wiley Interscience, New York, 1971) p. 245.
25. C. G. CANNON, *Spectrochim. Acta* **16** (1960) 302.
26. L. L. BLYLER and T. W. HAAS, *J. Appl. Polymer Sci.* **13** (1969) 2721.
27. J. J. POINT, M. DOSIERE, M. GILLOT and A. GOFFIN-GERIN, *J. Mater. Sci.* **6** (1971) 479.
28. S. GOGOLEWSKI and A. J. PENNINGS, *Polymer* **18** (1977) 650.
29. W. T. MEAD and R. S. PORTER, *J. Polymer Sci., Polymer Sci. Symp.* **63** (1978) 289.
30. T. HASHIMOTO, N. YASUDA, S. SUEHIRO, S. NOMURA and H. KAWAI, *A.S.C. Polymer Preprints* **17** (1976) 118.
31. W. PECHOLD, S. BLASENBREY and S. WOERNER, *Kolloid Z.* **189** (1963) 14.
32. P. E. McMAHON, R. L. McCULLOUGH and A. A. SCHLEGEL, *J. Appl. Phys.* **38** (1967) 4123.
33. D. H. RENEKER, *J. Polymer Sci.* **59** (1962) 539.
34. J. D. HOFFMAN, G. WILLIAMS and E. PASSAGLIA, *J. Polymer Sci.* **C-14** (1976) 173.
35. C. A. F. TUIJNMAN, *Polymer* **4** (1963) 259.
36. R. L. McCULLOUGH, *J. Macromol. Sci., Phys.* **9** (1974) 97.
37. A. PETERLIN, *J. Mater. Sci.* **6** (1971) 490.
38. R. E. ROBERTSON, *J. Polymer Sci., Polymer Phys. Ed.* **10** (1972) 2437.
39. A. E. TONELLI, in "Analytical Calorimetry" Vol. 3, edited by R. S. Porter and J. F. Johnson (Plenum Press, New York, 1974).
40. D. W. VAN KREVELEN and P. J. HOFTYZER, "Properties of Polymers" (Elsevier, Amsterdam, New York and Oxford, 1976) Ch. 4.
41. A. E. ZACHARIADES, P. D. GRISWOLD and R. S. PORTER, *Polymer Eng. Sci.* **19** (1979) 441.

Received 31 May and accepted 22 September 1980.